Geostatistical Analysis of Multiple Data Types that are not Available at the Same Locations

T. M. Wawruch (tmw@hixnet.co.za)
MinRED, AngloAmerican, Johannesburg, South Africa

C. V. Deutsch (cdeutsch@ualberta.ca)
University of Alberta, Edmonton, Alberta, Canada

J. A. McLennan (jam12@ualberta.ca)
University of Alberta, Edmonton, Alberta, Canada

Abstract

Geostatisticians commonly face modeling with multiple data types derived from different measurements of the same variable or measurements of different variables. These different data types are often non-isotopic, *that is, not available at the same locations. There are many examples of this complex data configuration in mining, environmental and petroleum geostatistics. If the objective is to make full use of all available information in constructing a model of coregionalization for subsequent estimation/simulation, it is necessary to calculate the cross-covariance between the different data types for all lag distances* **h***. Extrapolating the behavior of non-isotopic data to the expected behavior of collocated (***h***=0) data accounts for short-scale variability ignored in assuming collocation. The model of coregionalization and subsequent mapping will then makes full use of all available sample data information.*

Introduction

It is a rare luxury to conduct a geostatistical mapping exercise with only one variable measured with one sampling protocol/device. We are almost always faced with multiple variables, more than one sampling device and more than one sampling procedure. As a result, we are faced with modeling non-isotopic data. Isotopic sampling is when the multiple data variables are at the same location (Goovaerts, 1998). Some data are isotopic. For example, multiple grade or chemical assays on drill hole composites or porosity/permeability measurements from core plugs are isotopic. Nevertheless, there are many situations where we do not have isotopic samples:

- Two sampling campaigns with different sampling procedures, e.g. diamond drilling versus reverse circulation. Data of different vintages are collected with different sampling protocols, equipment and people at different times.
- Blast hole samples versus exploration drill hole samples. Blast hole samples represent a larger volume, incur a larger error in sample delimitation and extraction and are more prevalent than exploration samples.
- Geophysical measurements (seismic) may be collocated with well data, but may also be considered as data at different locations.

An ongoing problem of geostatistical analysis with non-isotopic or non-collocated samples is variogram calculation and modeling. The only practical model of coregionalization available is the Linear Model of Coregionalization (LMC). An LMC for two stationary variables, for example, requires, in addition to the two direct-variogram models, a cross-variogram or cross-covariance value at all distances and directions. Moreover, the cross-variogram cannot be calculated unless the data are collocated.

Consider two stationary variables Z and Y. The cross-variogram is calculated as follows for the LMC:

$$\gamma_{Z-Y}(\mathbf{h}) = \frac{1}{2 \cdot N(\mathbf{h})} \sum_{i=1}^{N(\mathbf{h})} \{[Z(\mathbf{u}_i) - Z(\mathbf{u}_i + \mathbf{h})][Y(\mathbf{u}_i) - Y(\mathbf{u}_i + \mathbf{h})]\} \tag{1}$$

The Z and Y data must be collocated, that is, the locations $\mathbf{u}_i$ and $\mathbf{u}_i$+**h**, $i = 1,..., N(\mathbf{h})$, where $N(\mathbf{h})$ is the number of Z-Y pairs separated by lag distances **h**, must have the complete set of both Z and Y variable values.

It is important to note at this point that the cross-covariance at lag distance **h**=0 ($C(\mathbf{0})$) is the sill of the cross-variogram while the cross-covariance for lag distances infinitesimally larger than 0 by some distance ε ($C(\varepsilon)$) accounts for the cross-variogram nugget effect. The two are not equivalent, that is, $C(\mathbf{0}) \neq C(\varepsilon)$.

Like all variogram modeling, a legitimate LMC requires judicious selection of geological rock types, treatment of trends and an appropriate coordinate space. Most orebodies permit some deterministic modeling of geological controls. Subsequent multivariate geostatistical estimation and simulation must consider all such interpretive geological information. This should not be forgotten in the following discussion.

A cross-variogram with non-isotopic data could only be calculated by assuming the samples are collocated. There are a number of problems with this approach. Consider the schematic illustration of Figure 1 with the non-isotopic x-o data configuration. When collocation is assumed, the variability for distances less than the smallest x-o lag distance **h** is not known and is not accounted for. The cross-covariance at lag **h**=0, which is the sill of the non-standardized cross-variogram, would thus be severely underestimated; it would be higher if the data truly were collocated. Thus, the difference between the different sampling methods or the two different variables is ignored. To avoid this misrepresentation of cross-covariance, nearby pairs, within some distance tolerance, can be assumed collocated. Figure 2 gives an example of this procedure using the x-o data configuration presented in Figure 1. This practice is also problematic. Although less severe than assuming collocation without a distance tolerance, short scale variability and/or the nugget effect may make the correlation seem poor when the variables could be, in fact, very well correlated.

The assumption of collocation for non-isotopic data makes the cross-variogram easy to calculate and the LMC straightforward to construct; however, there is no reason to pay with the inherent under evaluation of the cross-variogram sill. We would rather spend the additional professional time required to extrapolate the non-isotopic cross-covariance to that of collocated (**h**=0) cross-covariance.

The cross-covariance of two stationary non-isotopic variables Z and Y can be calculated and modeled for lag distances **h** greater than and equal to the minimum lag distance separating the paired Z-Y samples:

$$C_{Z-Y}(\mathbf{h}) = \frac{1}{N(\mathbf{h})} \sum_{i=1}^{N(\mathbf{h})} Z(\mathbf{u}_i) Y(\mathbf{u}_i + \mathbf{h}) \; - \; \frac{1}{N(\mathbf{h})} \sum_{i=1}^{N(\mathbf{h})} Z(\mathbf{u}_i) \cdot \frac{1}{N(\mathbf{h})} \sum_{i=1}^{N(\mathbf{h})} Y(\mathbf{u}_i + \mathbf{h}) \tag{2}$$

The cross-covariance calculation does not require collocated data. For distances less than the smallest **h**, however, the cross-covariance cannot be calculated using relation (2).

The cross-covariance model is completed for all **h** by an extrapolation procedure and an estimate of the nugget effect. The extrapolation procedure involves extrapolating the cross-covariance from **h** equal to the smallest distance separating the non-isotopic samples to **h** approaching 0. This contribution to the cross-covariance is referred to as the *structured cross-covariance contribution*. The cross-covariance at lags **h** smaller than what corresponds to the structured cross-covariance but infinitesimally larger than 0 by some distance ε, can be explained by an estimate of the nugget effect. A reasonable estimate of the relative cross-covariance/cross-variogram nugget effect is an average of the two direct-variogram relative nugget effects. The resulting nugget effect estimate also contributes to the cross-covariance. The cross-covariance at **h**=0, that is, the sill of the cross-variogram is calculated by adding the structured cross-covariance contribution to the cross-covariance contribution due to the nugget effect.

The sill estimate should be validated. The correlation coefficient associated to an estimated cross-variogram sill can be calculated and should agree with the correlation of the data as if it were collocated/isotopic. Uncertainty in the sill should also be evaluated. There is inherent uncertainty in all of the modeling parameters used to calculate the sill value and the impact of these uncertainties on the sill estimate should be assessed.

Knowing the sill of the cross-variogram and the model of cross-covariance for all lags **h**, the cross-variogram can be inferred. The LMC is then constructed so that subsequent cokriging and/or cosimulation accounts for the cross-covariance at all distances and directions **h**. The procedure effectively utilizes the full spatial potential of all the available sample information.

Theory

Consider two stationary variables Z and Y with means m_Z and m_Y and variances σ^2_Z and σ^2_Y. The variables are non-isotopic. A legitimate LMC takes on the following form:

$$\begin{aligned}
\gamma_{Z-Z}(\mathbf{h}) &= \sum_{i=0}^{nst} C^{(i)}_{Z-Z}\Gamma^{(i)}(\mathbf{h}) \\
\gamma_{Y-Y}(\mathbf{h}) &= \sum_{i=0}^{nst} C^{(i)}_{Y-Y}\Gamma^{(i)}(\mathbf{h}) \qquad i = 0,\ldots,nst \\
\gamma_{Z-Y}(\mathbf{h}) &= \sum_{i=0}^{nst} C^{(i)}_{Z-Y}\Gamma^{(i)}(\mathbf{h})
\end{aligned} \tag{3}$$

where

h is the separation distance or lag vector between *Z*-*Y* data pairs;

$\Gamma^{(i)}(\mathbf{h})$ are the i[th] nested structures, each defined by a variogram type, e.g. spherical, exponential, etc) and relevant anisotropy parameters. By convention, the 0[th] nested structure is the nugget effect;

the $C^{(i)}$ coefficients are variance contributions. They are constrained to ensure a positive definite LMC:

$$\left.\begin{array}{r} C^{(i)}_{Z-Z} \geq 0 \\ C^{(i)}_{Y-Y} \geq 0 \\ C^{(i)}_{Z-Z} C^{(i)}_{Y-Y} \geq (C^{(i)}_{Z-Y})^2 \end{array}\right\} i = 0,...,nst \tag{4}$$

the *Z*-*Z* and *Y*-*Y* direct-variograms and the *Z*-*Y* cross-variogram, $\gamma_{Z-Z}(\mathbf{h}), \gamma_{Y-Y}(\mathbf{h}), \gamma_{Z-Y}(\mathbf{h})$, respectively, are calculated as:

$$\begin{aligned} \gamma_{Z-Z}(\mathbf{h}) &= \frac{1}{2 \cdot N(\mathbf{h})} \sum_{i=1}^{N(\mathbf{h})} \{[Z(\mathbf{u}_i) - Z(\mathbf{u}_i + \mathbf{h})][Z(\mathbf{u}_i) - Z(\mathbf{u}_i + \mathbf{h})]\}; \\ \gamma_{Y-Y}(\mathbf{h}) &= \frac{1}{2 \cdot N(\mathbf{h})} \sum_{i=1}^{N(\mathbf{h})} \{[Y(\mathbf{u}_i) - Y(\mathbf{u}_i + \mathbf{h})][Y(\mathbf{u}_i) - Y(\mathbf{u}_i + \mathbf{h})]\}; \\ \gamma_{Z-Y}(\mathbf{h}) &= \frac{1}{2 \cdot N(\mathbf{h})} \sum_{i=1}^{N(\mathbf{h})} \{[Z(\mathbf{u}_i) - Z(\mathbf{u}_i + \mathbf{h})][Y(\mathbf{u}_i) - Y(\mathbf{u}_i + \mathbf{h})]\}; \end{aligned} \tag{5}$$

Since *Z* and *Y* are stationary and we assume $C_{Z-Y}(\mathbf{h}) = C_{Y-Z}(\mathbf{h})$, that is, there is no "lag effect":

$$\begin{aligned} \gamma_{Z-Z}(\mathbf{h}) &= C_{Z-Z}(\mathbf{0}) - C_{Z-Z}(\mathbf{h}) \\ \gamma_{Y-Y}(\mathbf{h}) &= C_{Y-Y}(\mathbf{0}) - C_{Y-Y}(\mathbf{h}) \\ \gamma_{Z-Y}(\mathbf{h}) &= C_{Z-Y}(\mathbf{0}) - C_{Z-Y}(\mathbf{h}) \end{aligned} \tag{6}$$

The Problem. The *Z* and *Y* variables are non-isotopic – the experimental cross-variogram $\gamma_{Z-Y}(\mathbf{h})$ cannot be calculated because the cross-variogram sill, or equivalently, the cross-covariance at **h**=0 is inaccessible and the cross-variogram nugget effect, or equivalently, the cross-covariance at **h**=ε is also inaccessible.

Proposed Approach. Calculate, plot and model $\gamma_{Z-Z}(\mathbf{h})$ and $\gamma_{Y-Y}(\mathbf{h})$. Observe the relative nugget effect in these models as $\frac{C^0_{Z-Z}}{\sigma^2_Z}$ and $\frac{C^0_{Y-Y}}{\sigma^2_Y}$, respectively (see Figure 3). Note the superscript "0" ($i = 0$) is used to represent the variance contribution due to the nugget effect.

Calculate, plot and model $C_{Z-Y}(\mathbf{h})$ for lag distances available from the data. In Figure 3, this corresponds to the x's modeled by the solid line on the cross-covariance plot. Extrapolate the cross-covariance (dotted line) to separation distances **h** approaching 0 to obtain the structured cross-covariance B_{Z-Y} (Although B_{Z-Y} contributes to the sill of the cross-variogram, it is not equal to the sill of the cross-variogram, $B_{Z-Y} \neq C_{Z-Y}(\mathbf{0})$, because it does not account for the *Z*-*Y* cross-covariance at **h**=ε, that is, the nugget effect.). We still need to estimate the cross-variogram nugget effect to access the cross-variogram sill. Our solution is to assume that the relative nugget effect of the cross-variogram, $\frac{C^0_{Z-Y}}{C_{Z-Y}(\mathbf{0})}$, is equal to the average relative nugget effect of the *Z* and *Y* direct-variograms:

$$\frac{C^0_{Z-Y}}{C_{Z-Y}(\mathbf{0})} = \frac{1}{2}\left(\frac{C^0_{Z-Z}}{\sigma^2_Z} + \frac{C^0_{Y-Y}}{\sigma^2_Y}\right) \quad (7)$$

The cross-variogram sill $C_{Z-Y}(\mathbf{0})$ can now be inferred. B_{Z-Y} and C^0_{Z-Y} are the structured cross-covariance and nugget effect of the non-standardized cross-variogram, respectively. They both contribute to the sill:

$$C_{Z-Y}(\mathbf{0}) = C^0_{Z-Y} + B_{Z-Y} \quad (8)$$

In this calculation, relation (7) is substituted for C^0_{Z-Y} leaving $C_{Z-Y}(\mathbf{0})$ as the only unknown:

$$C_{Z-Y}(\mathbf{0}) = \frac{B_{Z-Y}}{1 - \frac{1}{2}\left(\frac{C^0_{Z-Z}}{\sigma^2_Z} + \frac{C^0_{Y-Y}}{\sigma^2_Y}\right)} \quad (9)$$

The cross-variogram is now calculated:

$$\gamma_{Z-Y}(\mathbf{h}) = C_{Z-Y}(\mathbf{0}) - C_{Z-Y}(\mathbf{h}) \quad (10)$$

Relation (7) is the key to our approach. It allows us to infer the cross-covariance for infinitesimally small lags **h**=ε even though the data are separated by larger distances; however, it is reasonable that the relative nugget effect of the cross-variogram is between the relative nugget effects of the direct variograms. Recall relation (4) with the constraints on the $C^{(i)}$ variance contributions. The last constraint, $C^{(i)}_{Z-Z}C^{(i)}_{Y-Y} \geq (C^{(i)}_{Z-Y})^2, i = 0,...,nst$, limits the possible values for C^0_{Z-Y}. Given C^0_{Z-Z} and C^0_{Y-Y}, the upper bound of C^0_{Z-Y} is $\sqrt{C^0_{Z-Z} \cdot C^0_{Y-Y}}$ and the lower bound is 0. Since the domain of these bounds is consistent with a positive definite LMC, any estimate of C^0_{Z-Y} can be checked.

Validation

We must show that the cross-variogram sill estimate $C_{Z-Y}(\mathbf{0})$ is consistent with the isotopic correlation of the data. This cannot be proven in practice since the collocated data configuration would make our proposed approach unnecessary in the first place; however, we show that it works with an extensive example dataset. There is always uncertainty involved in extrapolating or fitting variogram parameters. Since the sill estimate $C_{Z-Y}(\mathbf{0})$ is a function of such parameters, it will also be uncertain. The magnitude of uncertainty in the sill must be assessed.

Correlation at h=0. A cross-plot of collocated *Z-Y* pairs will give the correlation at **h**=0. This is the true and maximum correlation of the data. And an estimated cross-variogram sill $C_{Z-Y}(\mathbf{0})$ is related to an estimate of the true (collocated) correlation:

$$\rho_{Z-Y}(\mathbf{0}) = \frac{C_{Z-Y}(\mathbf{0})}{\sqrt{\sigma_Z^2 \cdot \sigma_Y^2}} \tag{11}$$

Validation of $C_{Z-Y}(\mathbf{0})$ is based on the agreement of its associated correlation to the true *Z-Y* correlation (Accepting the structured cross-covariance B_{Z-Y} as the sill of the cross-variogram is incorrect – relation (11) shows that the associated correlation would be a severe underestimate of the true correlation. The cross-variogram sill $C_{Z-Y}(\mathbf{0})$ is the addition of the structured cross-covariance contribution B_{Z-Y} and the cross-covariance contribution due to the nugget effect C^0_{Z-Y} .).

Uncertainty in the Sill. From relation (9) it is clear that the cross-variogram sill estimate $C_{Z-Y}(\mathbf{0})$ is a function of five parameters:

$$C_{Z-Y}(\mathbf{0}) = f(C^0_{Z-Z}, C^0_{Y-Y}, \sigma_Z^2, \sigma_Y^2, B_{Z-Y}) \tag{12}$$

The uncertainty in each of the five parameters can be assigned using expert judgment – we know the direct-variogram sill parameters (σ_Z^2 and σ_Y^2) have low uncertainties since they are reliable one-point statistics and the extrapolated parameters (C^0_{Z-Z}, C^0_{Y-Y} and B_{Z-Y}) have higher uncertainties. An illustration of these 5 uncertainties is shown in Figure 4. A Monte Carlo approach can be used to transfer the 5 input uncertainties through to uncertainty in $C_{Z-Y}(\mathbf{0})$ and $\rho_{Z-Y}(\mathbf{0})$: A distribution is constructed for each parameter given its assigned uncertainty, a value from each of the 5 parameter distributions is drawn, these 5 values are input into relation (9) to obtain a sill estimate, the sill is then input into relation (11) to obtain the associated and the process is repeated a large number of times to create multiple realizations. Validation is based on the summary statistics of the resulting histograms of the sill and associated correlation realizations.

The theoretical and experimental link between the variance/covariance relationships will be applied to a poly-metallic sedimentary-exhalative deposit of lead and silver. The initial sampling campaign was based on collocated samples of two variables. This allows us to illustrate the proposed approach and validate the results.

An Example

The abundant dataset contains 52,080 2m composites of lead (Pb) and silver (Ag) over a 3500m by 500m area. Although this data configuration may not be available in practice, the methodology can only be checked with collocated data.

The collocated/isotopic Pb-Ag distribution is visualized in Figure 5. The true correlation between Pb and Ag is 0.82. The LMC is defined in order to quantify the Pb-Ag direct-variability and cross-variability. The three calculated and modeled variograms for the East-West direction and the resulting LMC modeling parameters are shown in Figure 6.

A non-isotopic database consisting of two datasets is now constructed. The first dataset is created by choosing 33,519 collocated samples of lead and silver (Pb1-Ag1); the second dataset is created by choosing 18,561 collocated samples of lead and silver (Pb2-Ag2). Both datasets approximate a regular grid covering the entire 3500m by 500m area; however, they are not available at the same locations, that is, they are non-isotopic. The 450m bench amongst both datasets is shown in Figure 7.

The proposed approach to variogram calculation and modeling with non-isotopic samples is demonstrated with the Pb1-Pb2 data and the Pb1-Ag2 data. The main East-West direction of continuity is presented and the variables are not standardized.

Pb1-Pb2. Typically, the correlation and sill of the Pb1-Pb2 cross-variogram would be accessed from a standard Pb1-Pb2 scatterplot assuming the samples are collocated. This plot is shown in Figure 8. We expect excellent correlation (1.0) since the Pb1 and Pb2 samples are from the same distribution (Pb). Ignoring the short-scale variability of the non-isotopic Pb1-Pb2 samples, however, significantly underestimates the correlation and cross-variogram sill to be 0.30.

In Figure 9, the calculated, plotted and modeled Pb1 and Pb2 direct-variograms are presented. The relative nugget effects of the latter are calculated as $\frac{C^0_{Pb1-Pb1}}{\sigma^2_{Pb1}} = \frac{34.0}{50.0}$ and $\frac{C^0_{Pb2-Pb2}}{\sigma^2_{Pb2}} = \frac{22.0}{40.0}$, respectively. The calculated Pb1-Pb2 cross-covariance $C_{Pb1-Pb2}(\mathbf{h})$ is also shown in Figure 9. The structured cross-covariance $B_{Pb1-Pb2}$ is extrapolated to 17.0. The relative nugget effect $\frac{C^0_{Pb1-Pb2}}{C_{Pb1-Pb2}(\mathbf{0})}$ of the cross-variogram is calculated as $\frac{1}{2}\left(\frac{34.0}{50.0} + \frac{22.0}{40.0}\right) = 0.615$. The sill of the Pb1-Pb2 cross-variogram $C_{Pb1-Pb2}(\mathbf{0})$ is then calculated as $\frac{17.0}{1-0.615} = 44.2$.

The link between covariance and correlation is now used to estimate the collocated Pb1-Pb2 correlation (expected to be 1.0). Using $\rho_{Pb1-Pb2}(\mathbf{0}) = \frac{C_{Pb1-Pb2}(\mathbf{0})}{\sqrt{\sigma^2_{Pb1} \cdot \sigma^2_{Pb2}}}$ with $C_{Pb1-Pb2}(\mathbf{0}) = 44.2, \sigma^2_{Pb1} = 50.0$ and $\sigma^2_{Pb2} = 40.0$, the theoretical correlation is 0.99.

Uncertainty in the parameters used for the cross-variogram sill calculation is now taken into account. Symmetric uncertainty of 1.0% for σ^2_{Pb1} and σ^2_{Pb2} and 3.0% for $C^0_{Pb1-Pb2}, C^0_{Pb2-Pb2}$ and $B_{Pb1-Pb2}$ were assumed. The uncertainty in the cross-covariance value $C_{Pb1-Pb2}(\mathbf{0}) = 44.2$ and associated correlation value $\rho_{Pb1-Pb2}(\mathbf{0}) = 0.99$ is assessed by constructing 10,000 Monte Carlo realizations of relations (9) and (11), respectively. The histograms of all such possible sill values and associated correlations are shown in Figure 10. The variance of each histogram is very low indicating that our estimates of 44.2 and 0.99 are very reliable given the assigned uncertainties.

Pb1-Ag2. A similar exercise is carried out with the non-isotopic Pb1-Ag2 data. By involving a second variable in the analysis, the expected correlation is no longer 1.0; we now expect the correlation to be that shown in Figure 5 (0.82). The scatter of Pb1-Ag2 pairs assuming collocation is shown in Figure 11. The Pb1-Ag2 correlation of 0.28 significantly underestimates the true correlation of 0.82.

The Pb1 and Ag2 direct-variograms and the Pb1-Ag2 cross-covariance model are presented in Figure 12. The structured Pb1-Ag2 cross-covariance and the relative Pb1-Ag2 nugget effect is extrapolated to 210.0 and calculated as 0.625, respectively. The sill of the cross-variogram is then found to be 560.0. The theoretical correlation corresponding to the sill estimate of 560.0 is calculated to be 0.82. This matches exactly the isotopic correlation shown in Figure 5. Using the same symmetric 1.0% uncertainty for the direct-variogram sills and the same 3.0% symmetric uncertainty for the extrapolated direct-variogram and structured cross-covariance parameters, the resulting uncertainty in the estimated sill value and its associated correlation estimate is assessed and displayed in Figure 13. Again, the variance of both histograms is very low indicating reliable estimates.

Discussion

We account for short-scale variability that is ignored in assuming collocation; however, reproduction of the correlation is extremely good in this example because of the large number of data. We expect some discrepancies between experimental and expected values when the variograms and cross-covariance models are not as well informed.

In a practical non-isotopic data setting, validation of the sill estimate would not be possible since the collocated data configuration is unknown. Nevertheless, if the goal is to make full use of all available information, the non-isotopic cross-covariance behavior must be extrapolated to cross-covariances smaller than the smallest non-isotopic data separation distance.

Assigning the relative cross-variogram nugget effect as the average relative nugget effect of the direct-variogram structures is crucial in our proposed approach. This method was not tested against other mineralogical settings. Uncommon trends or "lag" effects may invalidate the assumption implicit to relation (7); however, this assumption is consistent with physical intuition and a positive definite LMC. If the nugget effect in the cross-variogram is outside either direct-variogram nugget effects, the resulting LMC would not be positive definite and would not be "physically consistent". Further analysis is needed so that this proposed averaging technique can be applied to more general settings.

Implementation of the proposed approach is straightforward and repeatable. Any modest PC available at virtually any mine site can be used for implementation. The expert time required to implement the approach is minimal. Of course, we admit that cokriging and cosimulation is underutilized because of perceived difficulties in implementation.

The preceding discussion assumes a direct or Gaussian approach. Indicator geostatistics would require a different approach. Indicator cokriging or the Markov-Bayes algorithm could be adapted to the problem of non-isotopic sampling; however, the problem of inference would be more difficult.

Conclusion

Extrapolating non-isotopic cross-covariance to that of the expected collocated cross-covariance and estimating the cross-variogram nugget effect effectively solves the problem of geostatistical mapping with a Linear Model of Coregionalization. Cokriging and/or Cosimulation can be implemented so that the variability for all distances and directions is accounted for.

References

- Deutsch C.V., Journel A.G. (1998) *GSLIB: Geostatistical Software Library: and User's Guide* Oxford University Press, New York, 2nd Ed.
- Goovaerts, P. (1998) *Geostatistics for Natural Resources Evaluation*, Oxford University Press, New York.
- Journel, A.G. and Huijbregts, Ch.J., (1978) *Mining Geostatistics*, Academic Press, New York.
- A. Almeida and A. Journel. *Joint Simulation of Multiple Varibles With a Markov-Type Coregionalization Model*. Math Geology, 26(5):565-88, July 1994.
- J. Carr and D. Myers. *COSIM: A Fortran IV Program for Co-Conditional Simulation*. Computers & Geosciences, 11(6):675-705, 1985.
- D. Myers. *Cokriging – New Developments*. In G. Verly et al., editors, Geostatistics for Natural Resources Characterization, pages 295-305, Reidal, Dordrecht, Holland, 1984.
- H. Wackernagel. *Multivariate Geostatistics: An Introduction With Applications*. Springer-Verlag, Berlin, 1995.

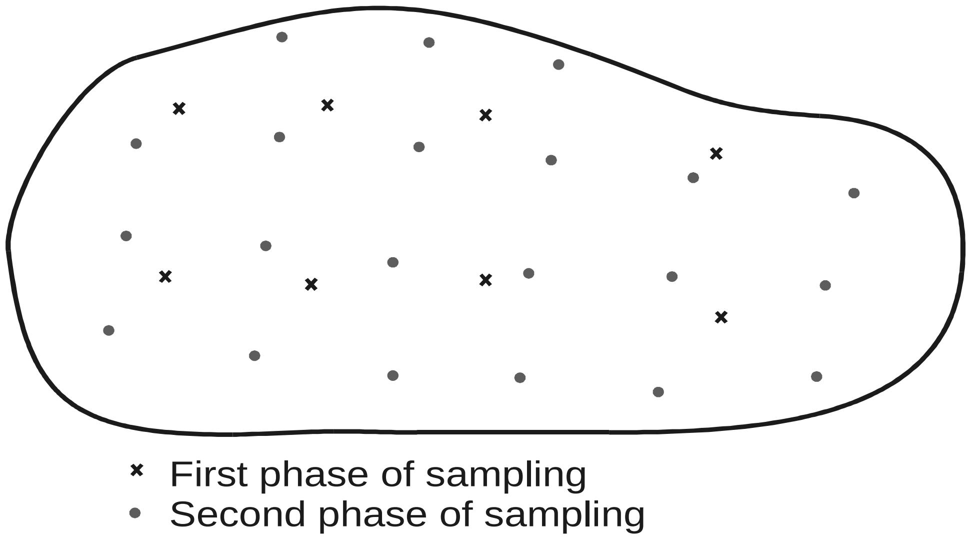

Figure 1 – Non-Isotopic Sampling. A schematic illustration of non-isotopic sampling. The x's and o's are not available at the same locations.

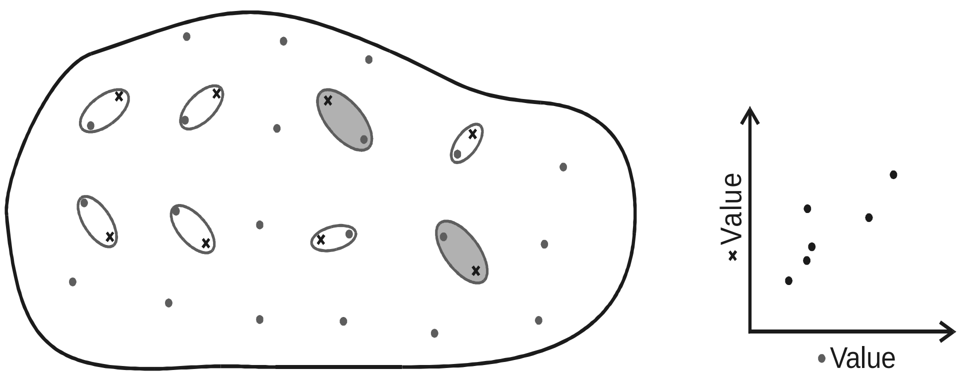

Figure 2 – Pairing Nearby Data. A schematic illustration of the common practice of pairing nearby data types. Samples are paired according to a distance tolerance (shown as the elliptical shapes). Six x-o pairs are deemed close enough (hollow ellipses), whereas two x-o pairs (shaded ellipses) are deemed too far apart. The six close x-o pairs are cross-plotted to infer the x-o cross-variogram sill.

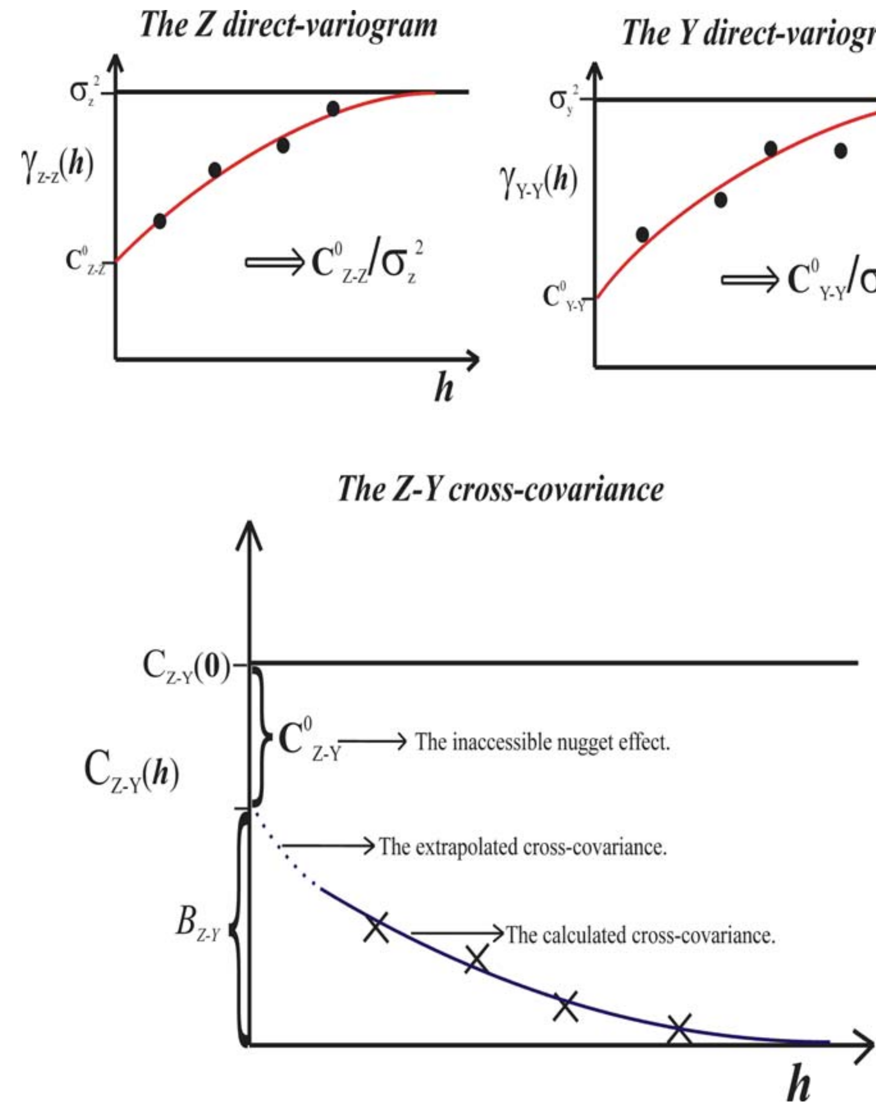

Figure 3 – The Proposed Approach. A graphic illustration of the parameters involved in the problem and proposed approach. The two direct-variograms, from which the relative nugget effects are to be calculated, are shown in the top. The calculated cross-covariance are the x's and the solid line is the model through them. The extrapolation to lag distances approaching 0 is shown by the dotted line.

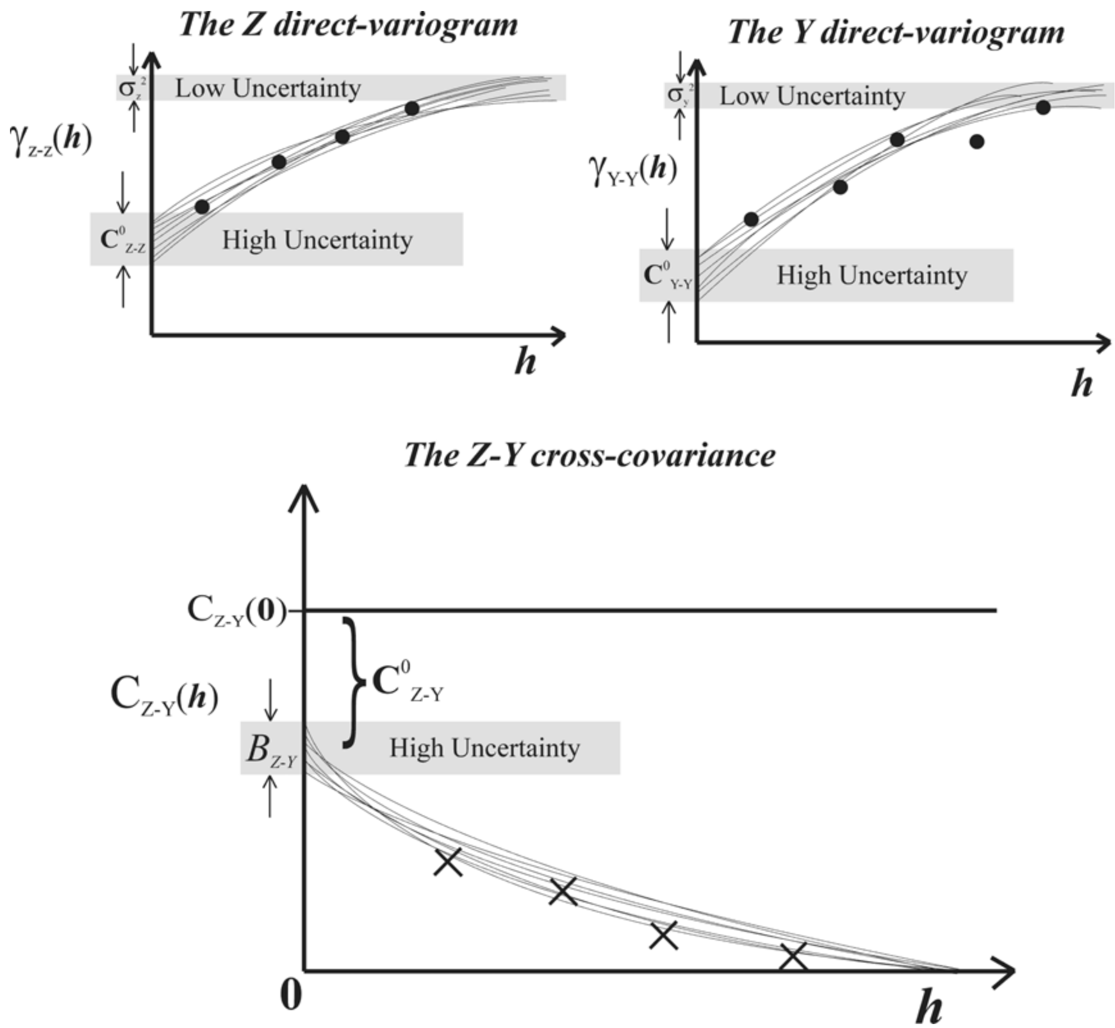

Figure 4 – Sill and Associated Correlation Uncertainty. A graphical illustration of the 5 parameter uncertainties relevant to the calculation of a sill estimate.

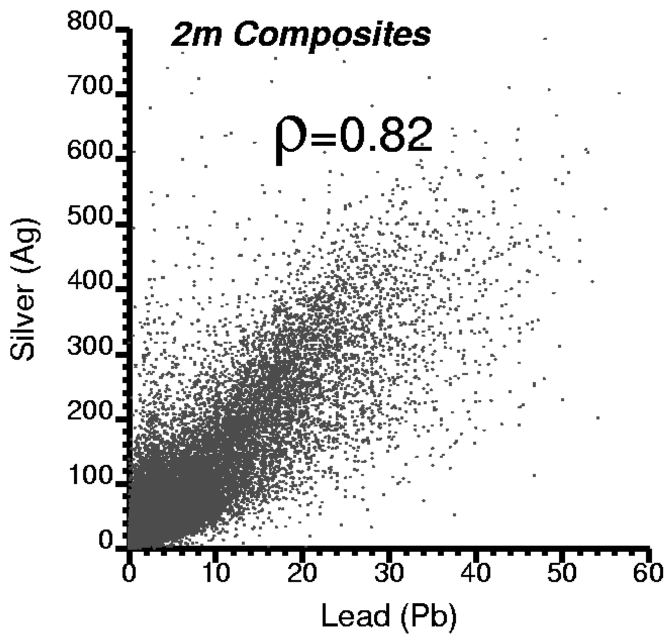

Figure 5 – Silver vs. Lead. The scatter of collocated Pb-Ag pairs showing a correlation of 0.82.

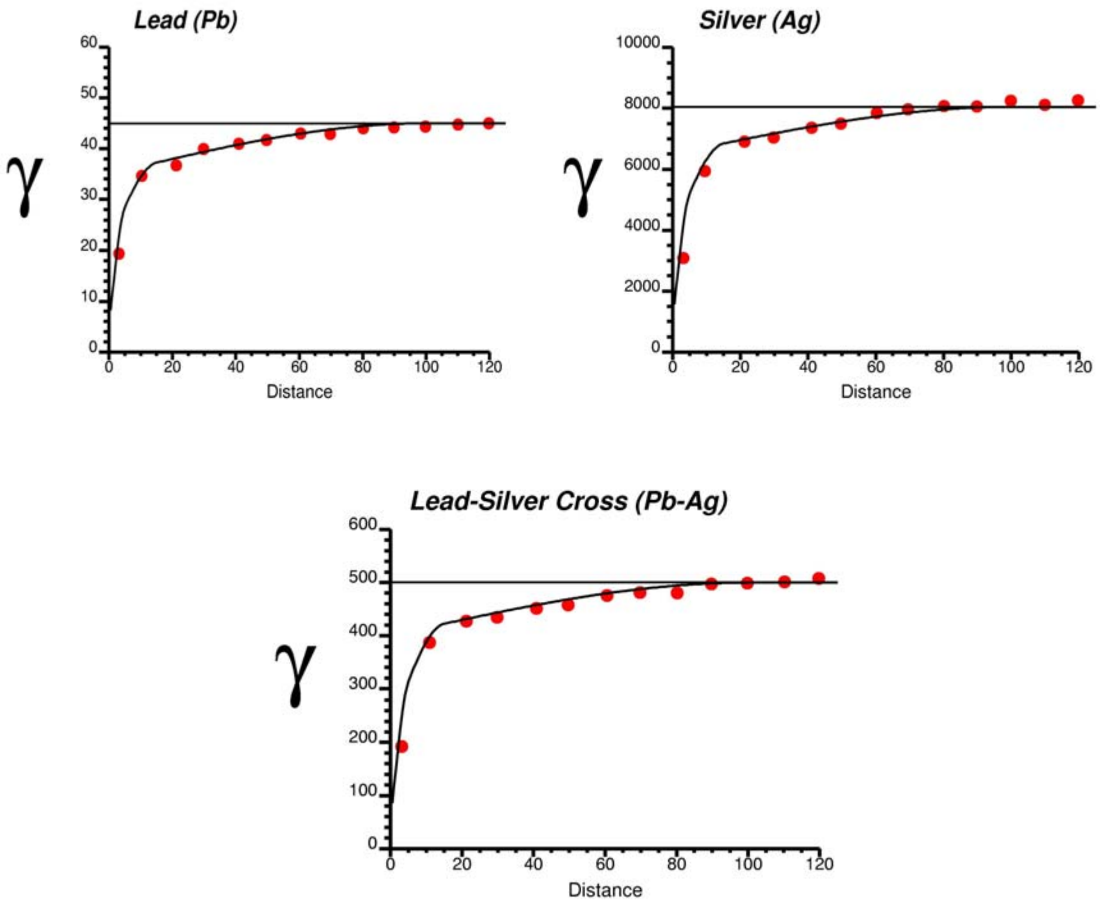

Variable	C_0	C_1	C_2	C_3	R_1	R_2	R_3
Pb-Ag	50	170	180	100	5	15	100
Pb	5	16	14	10	5	15	100
Ag	1000	2800	2700	1550	5	15	100

Figure 6 – LMC for Pb-Ag. The Pb-Ag Linear Model of Coregionalization (LMC) for the major East-West direction of continuity. For each structure of the three structures (not including the nugget effect), the variogram type is spherical, the *C* values are the variance contributions and the *R* (range) values define the deposit's anisotropy.

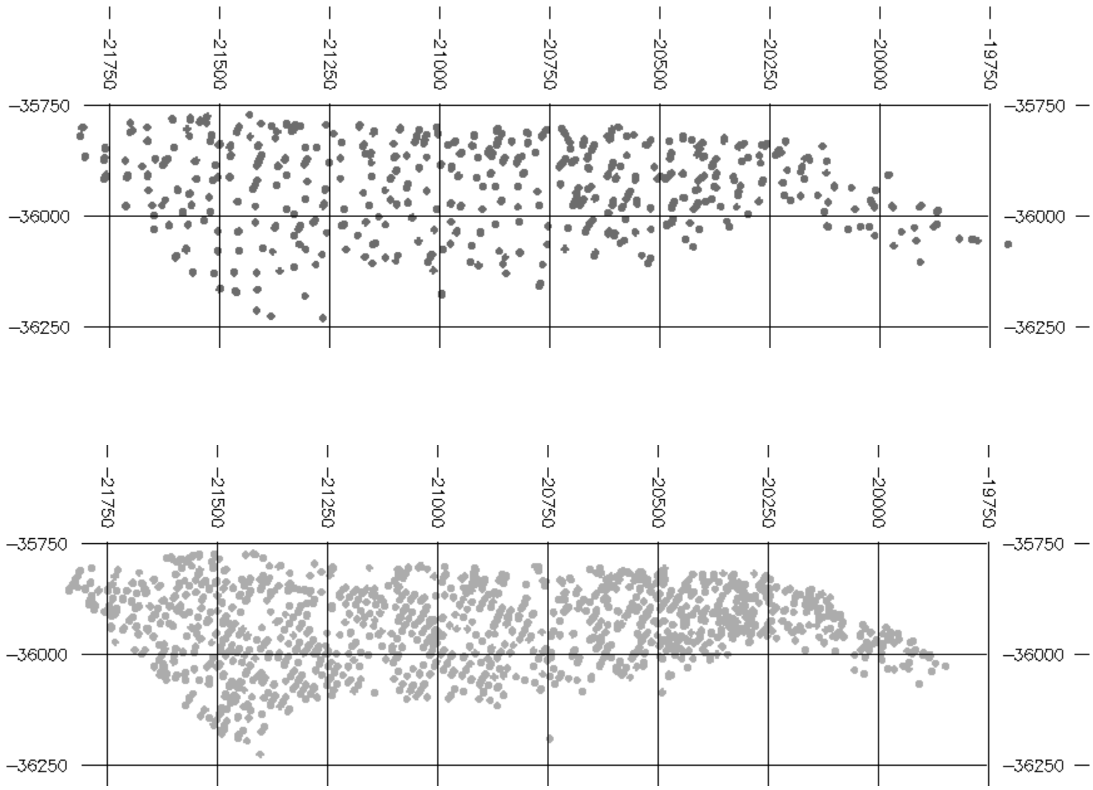

Figure 7 – Location of Pb1-Ag1 and Pb2-Ag2. The Pb1-Ag1 and Pb2-Ag2 data on the 450m bench. There are, in total, 33,519 samples of collocated Pb1 and Ag1 (top) and 18,561 collocated samples of Pb2 and Ag2 (bottom).

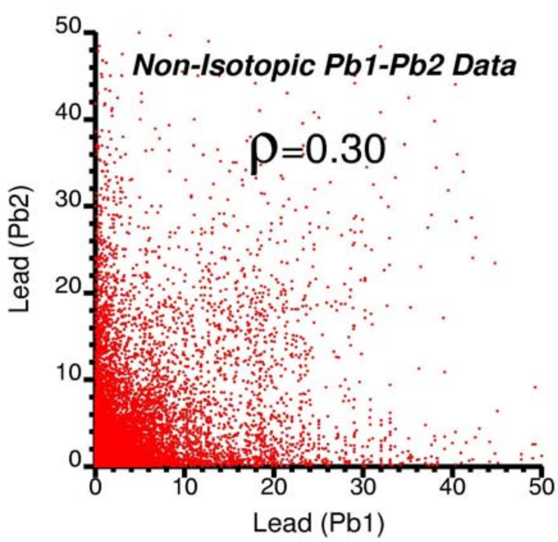

Figure 8 – Pb2 vs. Pb1. The scatter of non-isotopic Pb1-Pb2 pairs. The pairs are separated by **h**. The correlation of 0.30 is significantly lower than the expected correlation of 1.0.

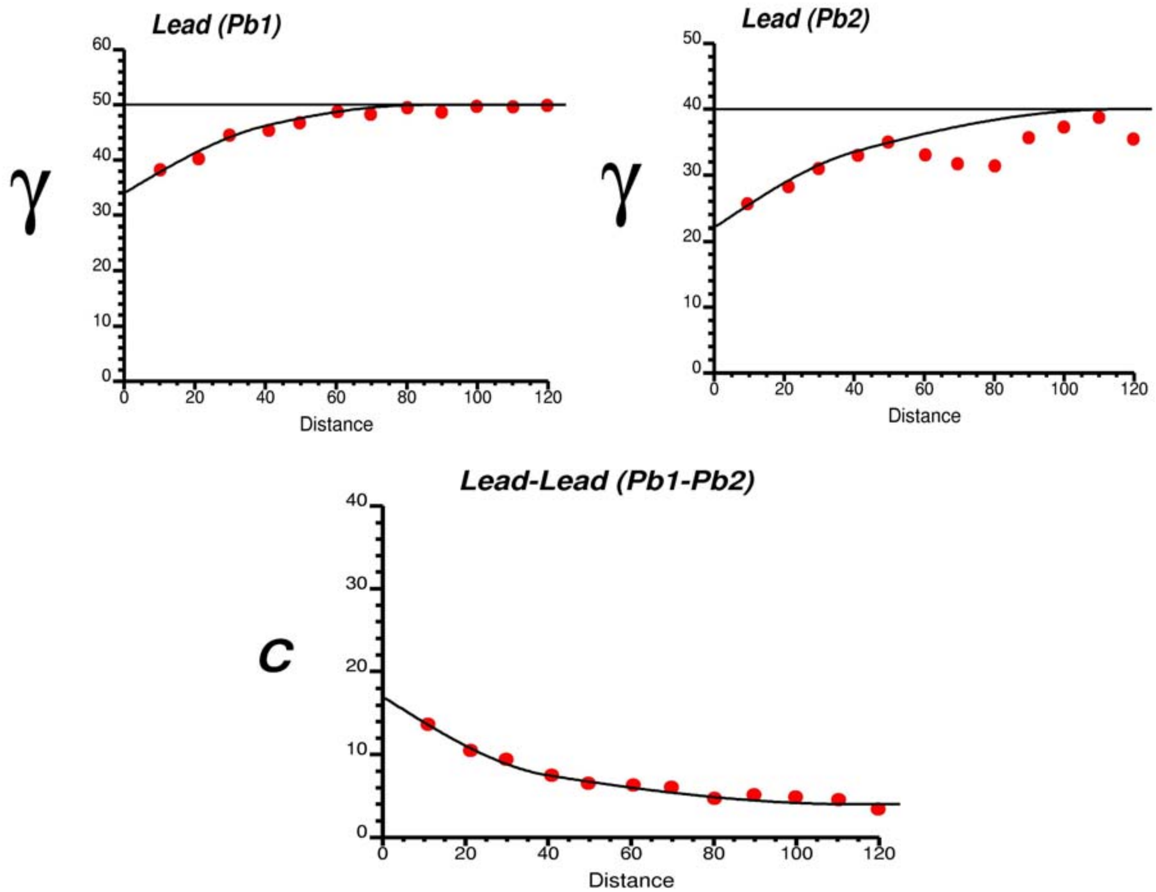

Figure 9 – Pb1-Pb2. The calculated and modeled direct Pb1 and Pb2 East-West direction direct-variograms along with a plot of the Pb1-Pb2 extrapolated cross-covariance model.

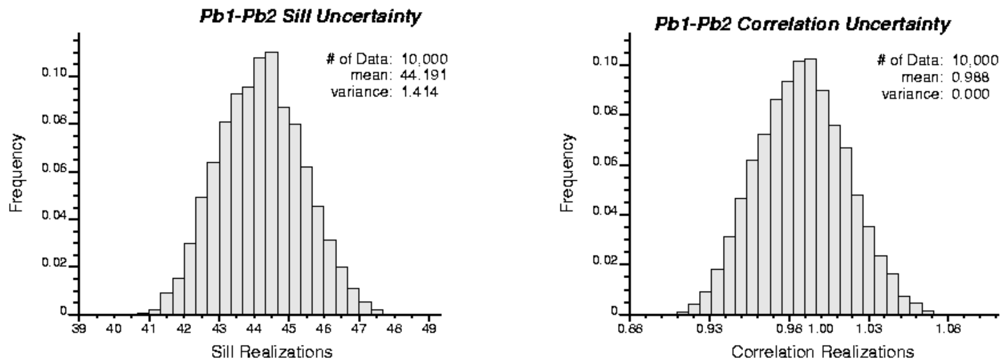

Figure 10 – Pb1-Pb2 Sill Uncertainty. The histograms of 10,000 realizations of the sill and associated correlation, given symmetric uncertainty of 1.0% in the direct-variogram sill parameters and 3.0% symmetric uncertainty in the extrapolated direct-variogram and cross-covariance modeling parameters. The variance of both distributions is low indicating the sill and associated correlation values are quite reliable.

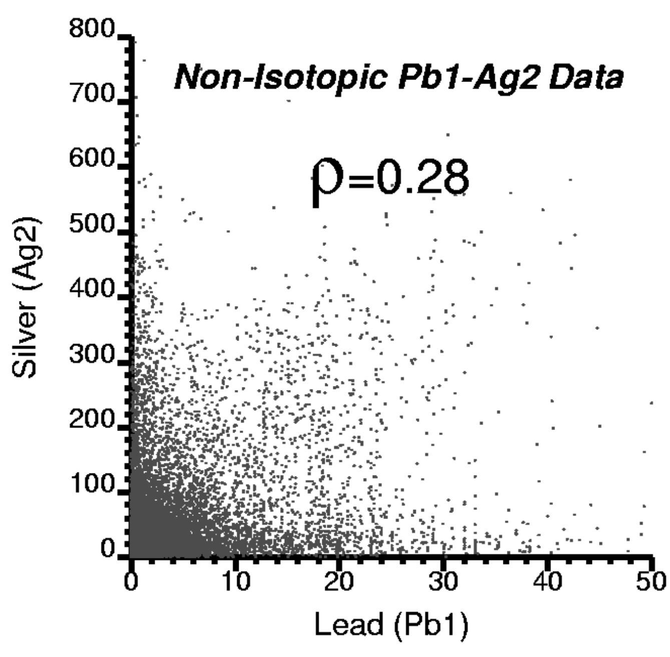

Figure 11 – Ag2 vs. Pb1. The scatter of non-isotopic Pb1-Ag2 pairs. The plotted pairs are separated by **h**. The correlation of 0.28 is significantly lower than the expected correlation of 0.82.

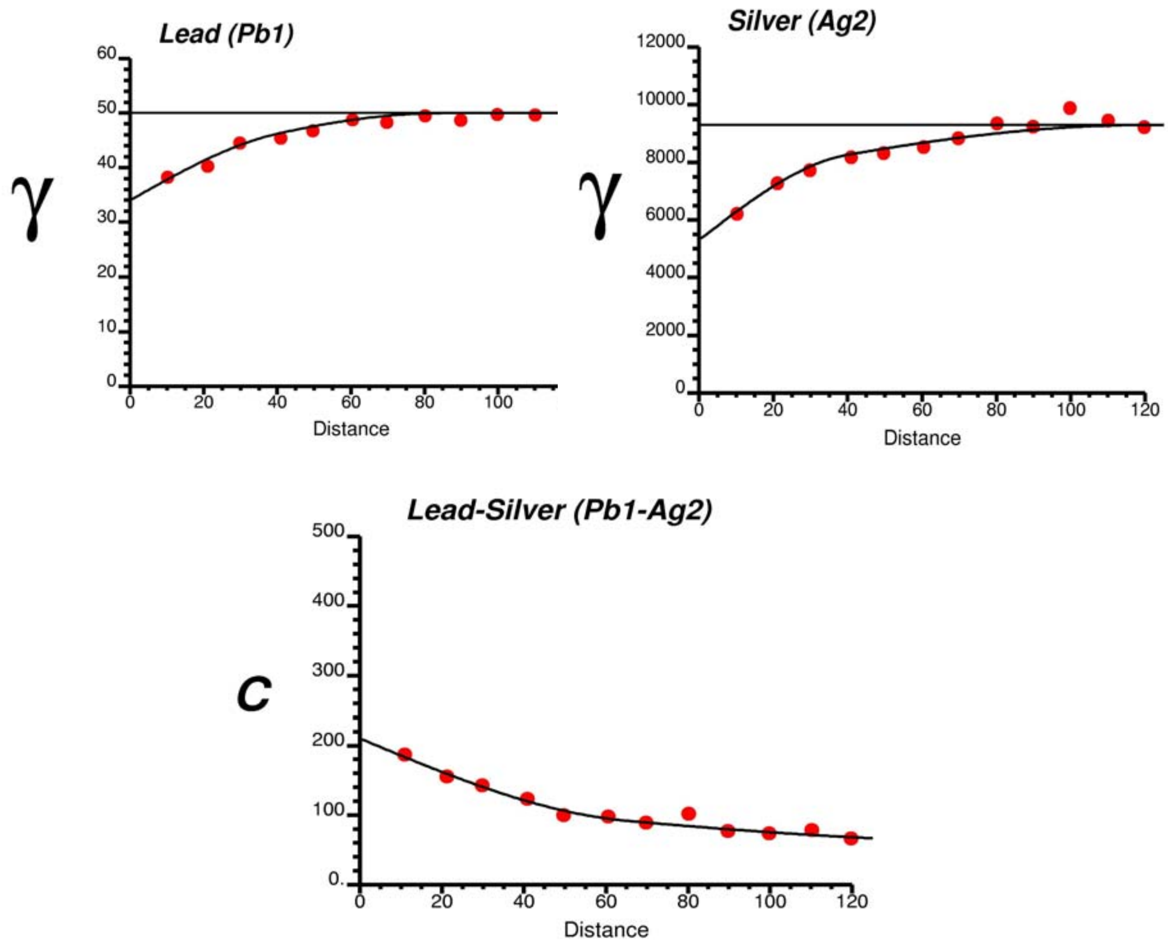

Figure 12 – Pb1-Ag2. The calculated and modeled direct Pb1 and Ag2 East-West direction direct-variograms along with the extrapolated Pb1-Ag2 cross-covariance model.

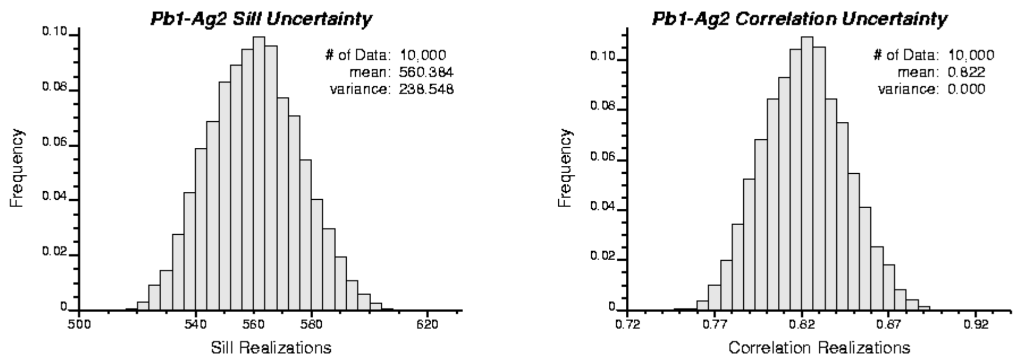

Figure 13 – Pb1-Ag2 Sill Uncertainty. The histograms of 10,000 realizations of the sill and associated correlation, using the same uncertainties for the same parameters as in the Pb1-Pb2 case. The variance of both distributions is quite low indicating that the sill and associated correlation estimates are reliable.